To appear in *Engineering Optimization*

Vol. 00, No. 00, Month 2015, 1–18

Online Supplement for 'Trust regions in Kriging-based optimization with expected improvement'

Rommel G. Regis*

Department of Mathematics, Saint Joseph's University, Philadelphia, USA

(*Received 8 December 2014; accepted 8 August 2015*)

Appendix A. Test problems for global optimization

Table A.1 shows the 18 lower-dimensional test problems (2 to 6 decision variables), which are the same ones used by Regis and Shoemaker (2013). Table A.2 shows the 10 higher-dimensional test problems with 30 or 32 decision variables.

Below are complete descriptions of the three 2-dimensional and three 3-dimensional Shekel test functions (Shekel2A, Shekel2B, Shekel2C, Shekel3A, Shekel3B, Shekel3C) and five instances of the Gordom–Wixom–Schoen (GWS) test function (Schoen 1993). The other test problems are well known and so their descriptions are found in many papers in the literature.

The 2-dimensional and 3-dimensional Shekel test problems have the same mathematical form as the Shekel problems in Dixon and Szegö (1978) except that the search space (the region defined by the bound constraints) has been rescaled to $[0, 1]^d$. In particular, they

*Corresponding author. Email: rregis@sju.edu

Table A.1. Lower-dimensional test problems for the computational experiments.

Test function	Dim	Domain	No. of local min's	No. of global min's	Global min value
Branin	2	$[-5,10]\times[0,15]$	3	3	0.398
Goldstein–Price	2	$[-2,2]^2$	4	1	3
GWSS_Spiked	2	$[0,1]^2$	≥ 24	1	5.0716
Shekel2A	2	$[0,1]^2$	5	1	-117.5507
Shekel2B	2	$[0,1]^2$	4	1	-115.0840
Shekel2C	2	$[0,1]^2$	4	1	-232.9396
Hartman3	3	$[0,1]^3$	4	1	-3.86
GWSS(3,10)	3	$[0,1]^3$	≥ 12	1	-82.6229
Shekel3A	3	$[0,1]^3$	3	1	-107.2426
Shekel3B	3	$[0,1]^3$	4	1	-217.8420
Shekel3C	3	$[0,1]^3$	4	1	-213.5834
GWSC(4,10)	4	$[0,1]^4$	≥ 12	1	-77.6950
Shekel5	4	$[0,10]^4$	5	1	-10.1532
Shekel7	4	$[0,10]^4$	7	1	-10.4029
Shekel10	4	$[0,10]^4$	10	1	-10.5364
GWSC(5,8)	5	$[0,1]^5$	≥ 6	1	-82.0265
Hartman6	6	$[0,1]^6$	4	1	-3.32
GWSS(6,8)	6	$[0,1]^6$	≥ 16	1	-61.1606

have the form

$$f(x) = -\sum_{i=1}^{k} \frac{1}{\|x - a_i\|^2 + c_i}, \quad x \in [0,1]^d, \tag{A1}$$

where $a_i \in [0,1]^d$ and $c_i \in \mathbb{R}$ for $i = 1, \ldots, k$. The various Shekel problems differ in the settings of the a_i's and c_i's in (A1). Let A be the matrix whose rows are the vectors $a_1, \ldots, a_m$ in row form and let C be a column vector whose entries are the values $c_1, \ldots, c_k$. The matrix A and vector C are given below for the various Shekel problems used. In addition, surface and contour plots of the 2-dimensional Shekel functions are shown in Figure A.1.

Table A.2. Higher-dimensional test problems for the computational experiments.

Test function	Dimensions	Domain	Global min value
Ackley	30	$[-15, 20]^d$	$-20 - \exp(1)$
Rastrigin	30	$[-4, 5]^d$	$-d$
Griewank	30	$[-500, 700]^d$	0
Keane	30	$[1, 10]^d$	< -0.39
Levy	30	$[-5, 5]^{30}$	< -11
Michalewicz	30	$[0, \pi]^{30}$	< -23
Extended Rosenbrock	30	$[-2, 2]^d$	0
Extended Powell Singular	32	$[-1, 3]^d$	0
Trigonometric	30	$[-1, 3]^d$	0
Broyden Tridiagonal	30	$[-1, 1]^d$	0

Shekel2A ($k = 5$)**:**

$$A = \begin{bmatrix} 0.20 & 0.30 \\ 0.80 & 0.15 \\ 0.50 & 0.40 \\ 0.30 & 0.70 \\ 0.70 & 0.82 \end{bmatrix} \qquad C = \begin{bmatrix} 0.01 \\ 0.04 \\ 0.02 \\ 0.03 \\ 0.02 \end{bmatrix}$$

Shekel2B ($k = 5$)**:**

$$A = \begin{bmatrix} 0.80 & 0.70 \\ 0.30 & 0.90 \\ 0.50 & 0.60 \\ 0.10 & 0.50 \\ 0.43 & 0.10 \end{bmatrix} \qquad C = \begin{bmatrix} 0.01 \\ 0.04 \\ 0.02 \\ 0.03 \\ 0.02 \end{bmatrix}$$

Shekel2C ($k = 10$)**:**

$$A = \begin{bmatrix} 0.5129 & 0.2802 \\ 0.2469 & 0.2730 \\ 0.4417 & 0.8765 \\ 0.7572 & 0.3955 \\ 0.1236 & 0.2535 \\ 0.2977 & 0.5538 \\ 0.4465 & 0.5888 \\ 0.1388 & 0.7462 \\ 0.5069 & 0.3522 \\ 0.8304 & 0.5726 \end{bmatrix} \qquad C = \begin{bmatrix} 0.0050 \\ 0.0150 \\ 0.0100 \\ 0.0075 \\ 0.0100 \\ 0.0150 \\ 0.0075 \\ 0.0150 \\ 0.0150 \\ 0.0075 \end{bmatrix}$$

Shekel3A ($k = 4$)**:**

$$A = \begin{bmatrix} 0.8622 & 0.6632 & 0.8631 \\ 0.5785 & 0.7726 & 0.4543 \\ 0.7695 & 0.5150 & 0.1178 \\ 0.4007 & 0.8189 & 0.4432 \end{bmatrix} \qquad C = \begin{bmatrix} 0.01 \\ 0.04 \\ 0.02 \\ 0.03 \end{bmatrix}$$

Shekel3B ($k = 4$)**:**

$$A = \begin{bmatrix} 0.5129 & 0.2802 & 0.2469 \\ 0.2730 & 0.4417 & 0.8765 \\ 0.7572 & 0.3955 & 0.1236 \\ 0.2535 & 0.2977 & 0.5538 \end{bmatrix} \qquad C = \begin{bmatrix} 0.005 \\ 0.020 \\ 0.010 \\ 0.015 \end{bmatrix}$$

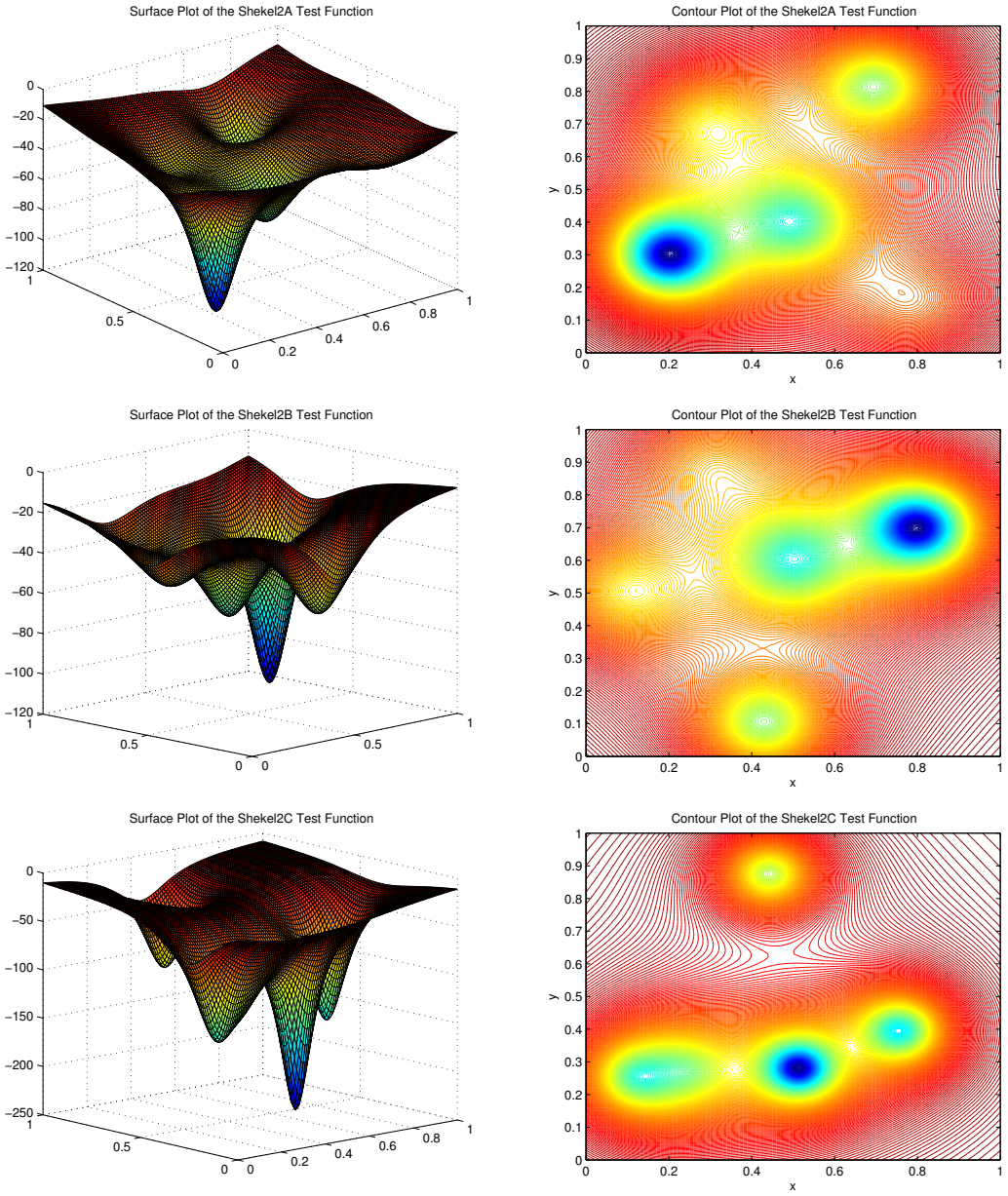

Figure A.1. Surface and contour plots of the two-dimensionial Shekel test functions.

Shekel3C ($k = 4$)**:**

$$A = \begin{bmatrix} 0.7911 & 0.8250 & 0.2601 \\ 0.6835 & 0.5342 & 0.4442 \\ 0.4171 & 0.2710 & 0.2070 \\ 0.8062 & 0.7518 & 0.6963 \end{bmatrix} \qquad C = \begin{bmatrix} 0.005 \\ 0.020 \\ 0.010 \\ 0.015 \end{bmatrix}$$

The Gordom–Wixom–Schoen (GWS) test functions (Schoen 1993) have the form

$$f(x) = \frac{\sum_{i=1}^{k} f_i \prod_{j \neq i} \|x - z_j\|^{\alpha}}{\sum_{i=1}^{k} \prod_{j \neq i} \|x - z_j\|^{\alpha}}, \quad x \in [0,1]^d, \tag{A2}$$

where $k \geq 1$; $z_j \in [0,1]^d$ for all $j = 1, \ldots, k$; and $f_i \in R$ for all $i = 1, \ldots, k$. The GWS test functions differ in the locations of $z_1, \ldots, z_k \in [0,1]^d$ and the values of $f_1, \ldots, f_k$. For convenience, let Z be the matrix whose rows are the vectors $z_1, \ldots, z_k$ in row form and F be the column vector whose entries are $f_1, \ldots, f_k$. The matrix Z and vector F are given below for the test problems used.

Four of the GWS test problems are labelled as GWSS(d, m) or GWSC(d, m) depending on whether $\alpha = 2$ or 3, respectively. The parameter m indicates the number of f_i's that are zero in (A2), which is equal to the number of f_i's that are strictly positive and also equal to the number of f_i's that are strictly negative. Hence, $k = 3m$ in (A2). The 2-dimensional GWSS_Spiked test function also has $\alpha = 2$ but used a different way to select the values of the f_i's. In particular, 25 of the 30 f_i's in the GWSS_Spiked function are set to a constant value while the remaining five are set to much lower values to create the spikes that can be seen in Figure A.2.

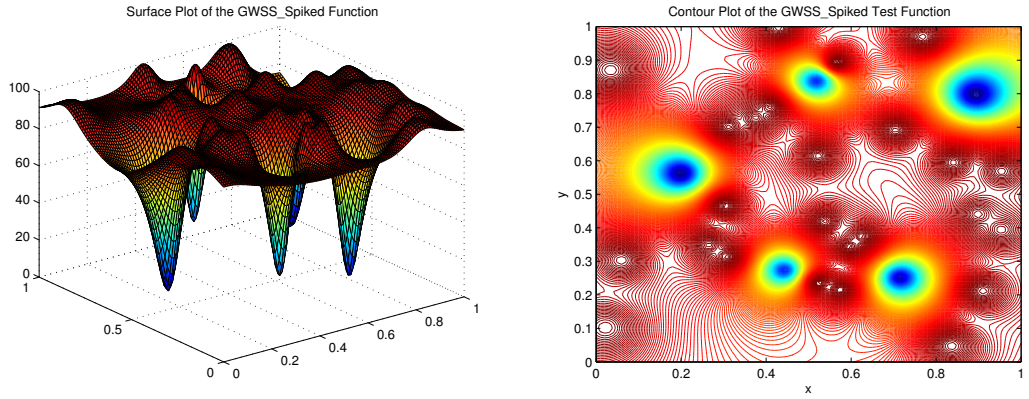

Figure A.2. Surface and contour plots of the GWSS_Spiked test function.

GWSS_Spiked ($k = 30,\ \alpha = 2$)**:**

$$Z = \begin{bmatrix} 0.9528 & 0.3945 \\ 0.7041 & 0.6916 \\ 0.9539 & 0.5693 \\ 0.5982 & 0.3432 \\ 0.8407 & 0.5949 \\ 0.4428 & 0.2739 \\ 0.8368 & 0.0481 \\ 0.5187 & 0.8381 \\ 0.0222 & 0.1025 \\ 0.3759 & 0.7283 \\ 0.8986 & 0.4405 \\ 0.4290 & 0.9972 \\ 0.1996 & 0.5625 \\ 0.3031 & 0.4659 \\ 0.5383 & 0.4190 \\ 0.9102 & 0.2116 \\ 0.5253 & 0.2358 \\ 0.3068 & 0.3141 \\ 0.0345 & 0.8699 \\ 0.7153 & 0.2518 \\ 0.7687 & 0.9696 \\ 0.0595 & 0.3033 \\ 0.6271 & 0.3740 \\ 0.2652 & 0.3484 \\ 0.3123 & 0.7008 \\ 0.5227 & 0.6144 \\ 0.4086 & 0.7592 \\ 0.8929 & 0.7991 \\ 0.5738 & 0.2156 \\ 0.5679 & 0.8936 \end{bmatrix} \qquad F = \begin{bmatrix} 100.0000 \\ 100.0000 \\ 100.0000 \\ 100.0000 \\ 100.0000 \\ 17.9940 \\ 100.0000 \\ 18.7823 \\ 100.0000 \\ 100.0000 \\ 100.0000 \\ 100.0000 \\ 5.4787 \\ 100.0000 \\ 100.0000 \\ 100.0000 \\ 100.0000 \\ 100.0000 \\ 100.0000 \\ 9.5413 \\ 100.0000 \\ 100.0000 \\ 100.0000 \\ 100.0000 \\ 100.0000 \\ 100.0000 \\ 100.0000 \\ 5.0716 \\ 100.0000 \\ 100.0000 \end{bmatrix}$$

GWSS(3,10) ($k = 30,\ \alpha = 2$)**:**

$$Z = \begin{bmatrix} 0.0340 & 0.7622 & 0.8760 \\ 0.4550 & 0.5506 & 0.3178 \\ 0.1286 & 0.1420 & 0.6606 \\ 0.2814 & 0.4114 & 0.7839 \\ 0.9909 & 0.7184 & 0.3167 \\ 0.2556 & 0.4116 & 0.1262 \\ 0.6009 & 0.3327 & 0.7224 \\ 0.8829 & 0.7581 & 0.4473 \\ 0.9658 & 0.3790 & 0.0724 \\ 0.7584 & 0.4773 & 0.6657 \\ 0.6737 & 0.8275 & 0.7715 \\ 0.1577 & 0.5911 & 0.0048 \\ 0.8711 & 0.4403 & 0.2539 \\ 0.0011 & 0.8616 & 0.4238 \\ 0.9111 & 0.5621 & 0.8025 \\ 0.2688 & 0.3543 & 0.4592 \\ 0.2356 & 0.9543 & 0.3161 \\ 0.7890 & 0.8863 & 0.0738 \\ 0.9421 & 0.1293 & 0.5527 \\ 0.7264 & 0.0972 & 0.2092 \\ 0.8417 & 0.0527 & 0.5263 \\ 0.2049 & 0.9310 & 0.6457 \\ 0.9524 & 0.0975 & 0.7275 \\ 0.4445 & 0.4960 & 0.5039 \\ 0.3548 & 0.0554 & 0.4826 \\ 0.7298 & 0.5767 & 0.2328 \\ 0.3166 & 0.0504 & 0.4855 \\ 0.1977 & 0.5599 & 0.7377 \\ 0.8740 & 0.4664 & 0.6528 \\ 0.8130 & 0.5938 & 0.4253 \end{bmatrix} \qquad F = \begin{bmatrix} -45.3638 \\ 0.0000 \\ 96.1173 \\ 0.0000 \\ 72.5092 \\ 0.0000 \\ 61.2896 \\ 0.0000 \\ 20.5799 \\ 21.7593 \\ 3.2423 \\ 51.1674 \\ 0.0000 \\ -43.0778 \\ -82.6229 \\ -38.9342 \\ -59.3494 \\ -22.3956 \\ -51.8049 \\ 0.0000 \\ 82.8175 \\ 98.7588 \\ 25.0732 \\ -12.5245 \\ -30.7533 \\ -78.1309 \\ 0.0000 \\ 0.0000 \\ 0.0000 \\ 0.0000 \end{bmatrix}$$

GWSC(4,10) ($k = 30,\ \alpha = 3$)**:**

$$Z = \begin{bmatrix} 0.8639 & 0.9168 & 0.8610 & 0.2135 \\ 0.9062 & 0.2649 & 0.9169 & 0.1578 \\ 0.2001 & 0.4788 & 0.6658 & 0.9454 \\ 0.8594 & 0.5117 & 0.3969 & 0.8253 \\ 0.7960 & 0.9492 & 0.3296 & 0.3603 \\ 0.3382 & 0.3264 & 0.5511 & 0.5193 \\ 0.7293 & 0.0593 & 0.6004 & 0.9032 \\ 0.5428 & 0.1309 & 0.0662 & 0.9939 \\ 0.4302 & 0.5937 & 0.1066 & 0.7815 \\ 0.3963 & 0.8801 & 0.2118 & 0.2802 \\ 0.2137 & 0.7117 & 0.2721 & 0.7747 \\ 0.1338 & 0.7837 & 0.7926 & 0.7401 \\ 0.8827 & 0.3871 & 0.2643 & 0.4165 \\ 0.8147 & 0.4638 & 0.4651 & 0.3018 \\ 0.7453 & 0.9219 & 0.0105 & 0.4354 \\ 0.9760 & 0.5044 & 0.6193 & 0.0834 \\ 0.1243 & 0.0531 & 0.5417 & 0.5649 \\ 0.6313 & 0.7718 & 0.4539 & 0.3098 \\ 0.9310 & 0.8438 & 0.7118 & 0.0037 \\ 0.8655 & 0.7055 & 0.5973 & 0.0836 \\ 0.5012 & 0.2078 & 0.3872 & 0.7023 \\ 0.5047 & 0.2683 & 0.7752 & 0.8661 \\ 0.9838 & 0.7215 & 0.3238 & 0.8627 \\ 0.8423 & 0.7420 & 0.0435 & 0.0443 \\ 0.4512 & 0.8572 & 0.9084 & 0.7122 \\ 0.3200 & 0.5363 & 0.8751 & 0.1172 \\ 0.2344 & 0.7854 & 0.7039 & 0.7229 \\ 0.7682 & 0.6795 & 0.9753 & 0.6862 \\ 0.3214 & 0.8172 & 0.2669 & 0.9425 \\ 0.5533 & 0.3912 & 0.6763 & 0.6395 \end{bmatrix} \qquad F = \begin{bmatrix} 87.0732 \\ 0.0000 \\ 0.0000 \\ -55.1071 \\ 38.3117 \\ 24.5952 \\ -59.0031 \\ 73.8706 \\ 43.9404 \\ -36.3970 \\ -61.3825 \\ -24.2549 \\ -4.0881 \\ 0.0000 \\ -40.3207 \\ -69.9486 \\ 74.4196 \\ 0.0000 \\ 16.7437 \\ 0.0000 \\ -12.5904 \\ 0.0000 \\ -77.6950 \\ 0.0000 \\ 32.5101 \\ 0.0000 \\ 58.2974 \\ 0.0000 \\ 0.0000 \\ 77.5639 \end{bmatrix}$$

GWSC(5,8) ($k = 24,\ \alpha = 3$)**:**

$$Z = \begin{bmatrix} 0.4360 & 0.7125 & 0.1941 & 0.4489 & 0.9355 \\ 0.8212 & 0.2070 & 0.5406 & 0.3723 & 0.6939 \\ 0.6647 & 0.2199 & 0.9843 & 0.8336 & 0.0788 \\ 0.6455 & 0.9383 & 0.2480 & 0.4243 & 0.7790 \\ 0.8440 & 0.9577 & 0.1796 & 0.6700 & 0.8217 \\ 0.9494 & 0.6843 & 0.4770 & 0.7571 & 0.3592 \\ 0.4117 & 0.6776 & 0.4858 & 0.3263 & 0.7966 \\ 0.8330 & 0.3141 & 0.4633 & 0.7735 & 0.2015 \\ 0.4823 & 0.9189 & 0.8416 & 0.9458 & 0.7930 \\ 0.0122 & 0.1267 & 0.7922 & 0.8874 & 0.3992 \\ 0.8976 & 0.9420 & 0.3832 & 0.6918 & 0.9980 \\ 0.2568 & 0.8988 & 0.6805 & 0.8703 & 0.7841 \\ 0.5712 & 0.8053 & 0.0101 & 0.6428 & 0.0708 \\ 0.1402 & 0.3844 & 0.8186 & 0.0202 & 0.5324 \\ 0.1228 & 0.8544 & 0.1602 & 0.4931 & 0.3691 \\ 0.5377 & 0.9558 & 0.8483 & 0.2906 & 0.4811 \\ 0.4879 & 0.2571 & 0.6513 & 0.0050 & 0.9713 \\ 0.4782 & 0.5496 & 0.2620 & 0.3920 & 0.7429 \\ 0.5013 & 0.5147 & 0.8613 & 0.6519 & 0.4914 \\ 0.2307 & 0.6180 & 0.0885 & 0.0650 & 0.1584 \\ 0.6298 & 0.3369 & 0.1805 & 0.3586 & 0.3154 \\ 0.3951 & 0.5940 & 0.7457 & 0.8579 & 0.7829 \\ 0.9319 & 0.8099 & 0.3956 & 0.7169 & 0.9487 \\ 0.5286 & 0.1336 & 0.3184 & 0.4277 & 0.1304 \end{bmatrix} \qquad F = \begin{bmatrix} -20.4633 \\ 33.0320 \\ 17.5600 \\ 0.0000 \\ 0.0000 \\ 0.0000 \\ -22.5134 \\ 13.5569 \\ -15.2171 \\ 93.9229 \\ 38.0815 \\ -27.2901 \\ 0.0000 \\ -14.0894 \\ 20.7970 \\ 0.0000 \\ -21.7164 \\ -73.7243 \\ 0.0000 \\ 54.6899 \\ -82.0265 \\ 97.5947 \\ 0.0000 \\ 0.0000 \end{bmatrix}$$

GWSS(6,8) ($k = 24,\ \alpha = 2$)**:**

$$Z = \begin{bmatrix}
0.5162 & 0.7379 & 0.3853 & 0.5854 & 0.2267 & 0.1560 \\
0.2252 & 0.5115 & 0.1863 & 0.9370 & 0.1161 & 0.4260 \\
0.1837 & 0.1949 & 0.2248 & 0.9935 & 0.7173 & 0.8230 \\
0.2163 & 0.8676 & 0.9119 & 0.8705 & 0.3684 & 0.0512 \\
0.4272 & 0.6341 & 0.9859 & 0.8706 & 0.7627 & 0.0003 \\
0.9706 & 0.3952 & 0.0440 & 0.1909 & 0.3367 & 0.6182 \\
0.8215 & 0.8975 & 0.3183 & 0.7651 & 0.7153 & 0.8464 \\
0.3693 & 0.1835 & 0.5199 & 0.4229 & 0.1740 & 0.7469 \\
0.0295 & 0.0216 & 0.3339 & 0.5156 & 0.3343 & 0.5611 \\
0.1919 & 0.0909 & 0.7236 & 0.5917 & 0.6921 & 0.8822 \\
0.2471 & 0.5217 & 0.1274 & 0.7005 & 0.9175 & 0.1685 \\
0.5672 & 0.3342 & 0.9158 & 0.0203 & 0.0314 & 0.5742 \\
0.4331 & 0.4341 & 0.2758 & 0.1118 & 0.9688 & 0.2095 \\
0.6111 & 0.2847 & 0.4526 & 0.7944 & 0.3442 & 0.9437 \\
0.0485 & 0.6537 & 0.6820 & 0.1223 & 0.6459 & 0.8577 \\
0.8077 & 0.1906 & 0.1734 & 0.3500 & 0.2309 & 0.4356 \\
0.5087 & 0.0641 & 0.1280 & 0.8652 & 0.0811 & 0.8314 \\
0.3153 & 0.2679 & 0.4267 & 0.2577 & 0.3129 & 0.9364 \\
0.9130 & 0.8259 & 0.0844 & 0.2799 & 0.4228 & 0.7448 \\
0.5907 & 0.3353 & 0.7979 & 0.2283 & 0.4011 & 0.5845 \\
0.5751 & 0.9650 & 0.0073 & 0.8963 & 0.1349 & 0.4318 \\
0.0003 & 0.2957 & 0.6648 & 0.3541 & 0.7697 & 0.5519 \\
0.1592 & 0.3813 & 0.9881 & 0.8885 & 0.4700 & 0.7304 \\
0.2749 & 0.6237 & 0.3090 & 0.0224 & 0.3706 & 0.7959
\end{bmatrix}$$

$$F = \begin{bmatrix}
0.0000 \\
40.3002 \\
-12.5135 \\
-53.1524 \\
52.8257 \\
-61.1606 \\
0.0000 \\
0.0000 \\
0.0000 \\
0.0000 \\
-33.9558 \\
-33.2600 \\
0.0000 \\
-4.8386 \\
70.6070 \\
-28.0004 \\
62.2734 \\
97.0148 \\
26.5811 \\
95.4861 \\
-29.0180 \\
0.0000 \\
5.5993 \\
0.0000
\end{bmatrix}$$

Appendix B. Management of groundwater bioremediation

The TRIKE and CYCLONE algorithms are also compared with standard EGO on a 36-dimensional groundwater bioremediation problem (Yoon and Shoemaker 1999). Groundwater bioremediation is the process of promoting the growth of soil bacteria that can transform groundwater contaminants into harmless substances. This study uses the optimization formulation in Yoon and Shoemaker (1999), which considers a setup that pumps oxygenated water into the groundwater by means of injection wells and uses monitoring wells to measure contaminant concentrations at specific locations. The optimization formulation uses a two-dimensional finite element simulation model that describes groundwater flow and changes in the concentrations of the contaminant, oxygen and biomass. The entire planning horizon is divided into management periods and the goal is to determine the pumping rates for each injection well at the beginning of each management

period that minimize the total pumping cost subject to the constraint that the contaminant concentrations at the monitoring wells are below a certain threshold during specified time periods. In Yoon and Shoemaker (1999), the constraints are incorporated into the total pumping cost objective function via a penalty term, resulting in a bound constrained global optimization problem.

This groundwater bioremediation model uses a hypothetical contaminated aquifer described in Yoon and Shoemaker (1999) whose characteristics are symmetric about a horizontal axis. There are six injection wells that are also symmetrically arranged such that pumping decisions are only needed on the three injection wells on one side of the axis of symmetry. There are 12 management periods (where each management period is a month), giving $12 \times 3 = 36$ decision variables. The decision variables are scaled so that the search space is $[0, 1]^{36}$. This groundwater bioremediation problem is referred to as GWB36.

The simulation time for this groundwater bioremediation model is only about 0.1 second on an Intel® Core™ i7 CPU 860 2.8 GHz desktop PC. However, the above optimization problem is representative of computationally expensive groundwater bioremediation problems, whose simulation times can take a few minutes to many hours depending on the complexity of the model.

Appendix C. Effects of the localization and restart strategies

Figure C.1 shows the average of the minimum distance of the current sample point from previous sample points after every function evaluation for EGO, CYCLONE and TRIKE on the Shekel5, Shekel7, GWSC(5,8) and Hartman6 functions. The corresponding plots for Shekel10 and GWSS(6,8) are included in the main manuscript.

Table C.1 shows the MLEs for the success probabilities of CYCLONE and TRIKE (stopped when $\epsilon_{\text{EI}} < 0.001$) within CYCLONE-Restart and TRIKE-Restart, respectively.

Appendix D. Comparison of progress curves on the higher-dimensional test problems

Figures D.3[**AQ10**] show the average progress curves for each algorithm on each of the higher-dimensional test problems as the number of function evaluations increases. The corresponding plot for the groundwater application is included in the main article. As mentioned before, the error bars are 95% t-confidence intervals for the mean. That is, the length of each side of the error bar is equal to 2.045 times the standard deviation of the

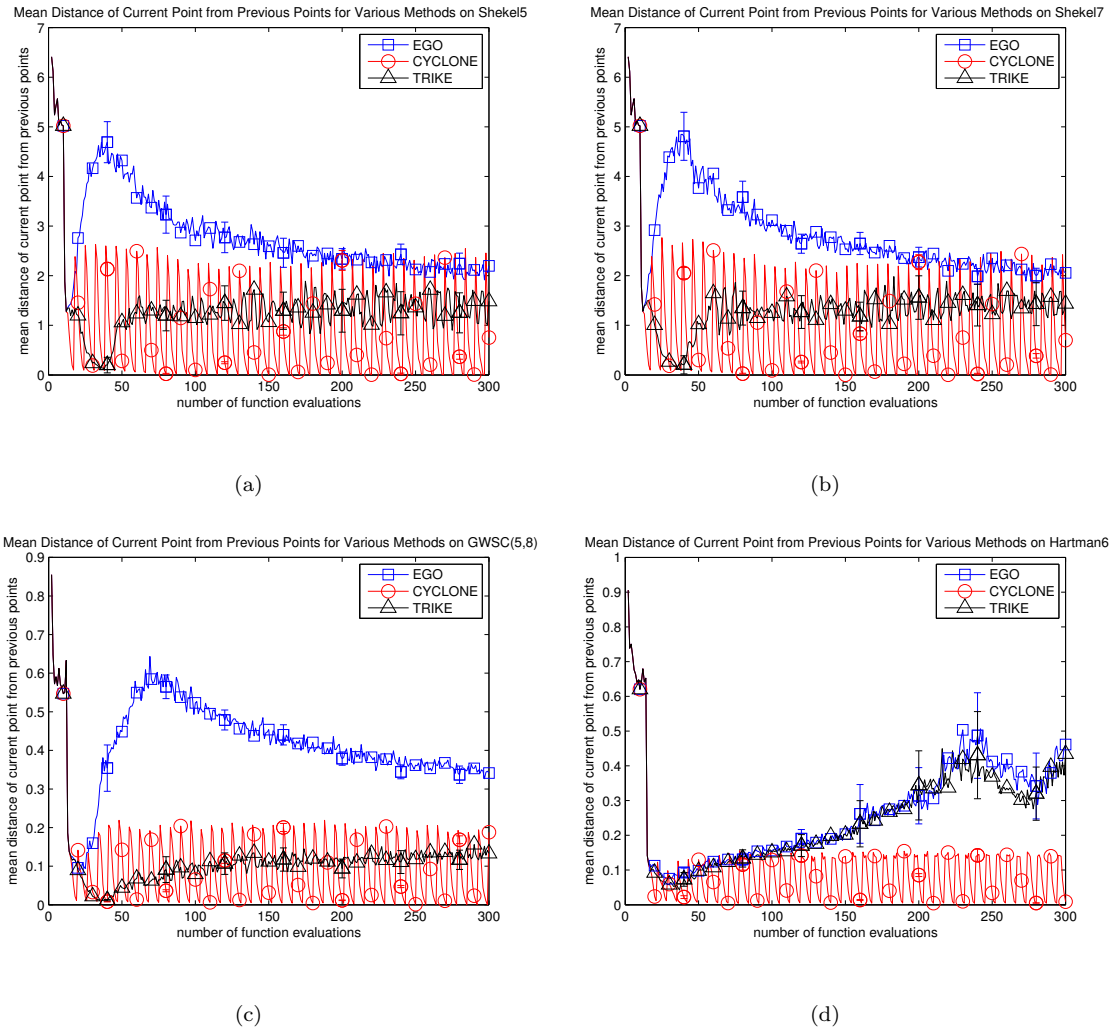

Figure C.1. Mean (over trials) of the minimum distance of the current point from previous points versus number of function evaluations for EGO, CYCLONE and TRIKE. Error bars represent 95% t-confidence intervals for the mean.

Table C.1. Maximum likelihood estimates of the probability of getting within 1% of the global minimum value for each run of CYCLONE and TRIKE within CYCLONE-Restart and TRIKE-Restart, respectively.

Test problem	CYCLONE-Restart	TRIKE-Restart	Test problem	CYCLONE-Restart	TRIKE-Restart
Branin	0.81	0.64	Shekel3B	0.45	0.50
GP	0.71	0.58	Shekel3C	0.47	0.28
GWSS_Spiked	0.21	0.33	GWSC(4,10)	0.50	0.39
Shekel2A	0.54	0.70	Shekel5	0.31	0.22
Shekel2B	0.27	0.34	Shekel7	0.37	0.33
Shekel2C	0.45	0.43	Shekel10	0.40	0.36
Hartman3	0.79	0.83	GWSC(5,8)	0.39	0.45
GWSS(3,10)	0.24	0.17	Hartman6	0.67	0.71
Shekel3A	0.29	0.32	GWSS(6,8)	0.32	0.28

best function value divided by the square root of the number of trials. The factor 2.045 is the critical value corresponding to a 95% confidence level for a t-distribution with 29 degrees of freedom.

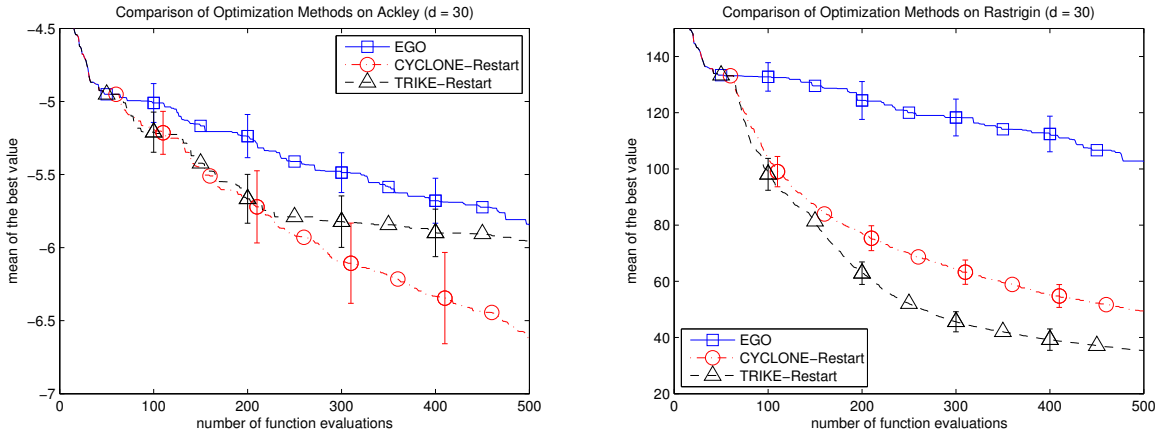

(a) (b)

Figure D.1. Average progress curves of TRIKE-Restart and CYCLONE-Restart on the 30-dimensional test problems with large numbers of local minima. The averages are taken for 30 trials corresponding to 30 different starting points. Error bars represent 95% t-confidence intervals for the mean.

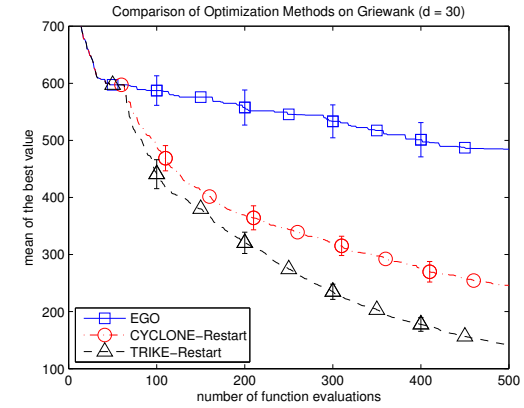

(a)

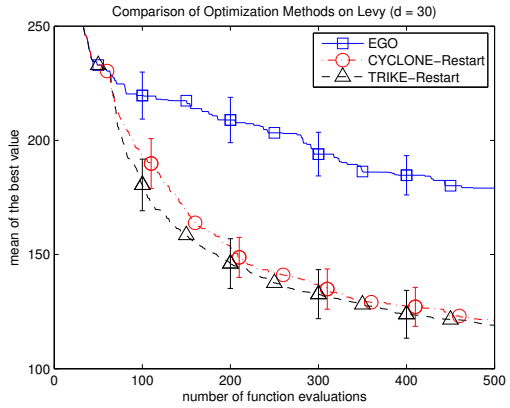

(b)

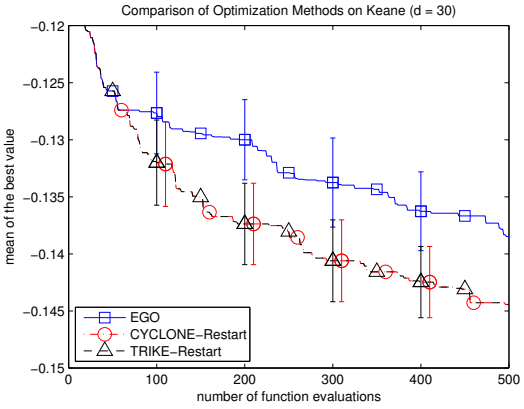

(c)

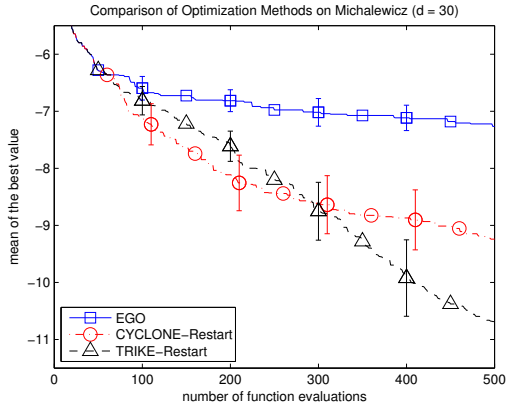

(d)

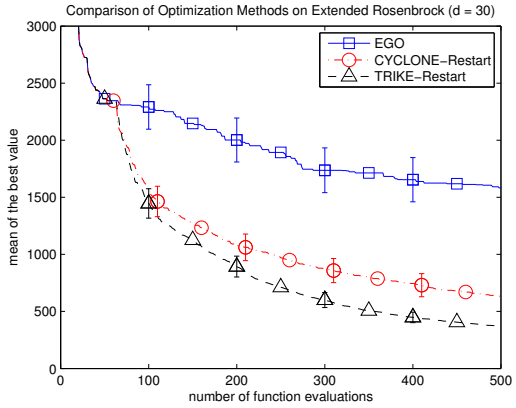

(e)

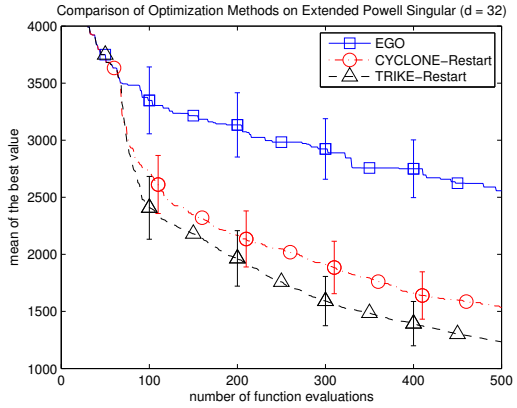

(f)

Figure D.2. Average progress curves of TRIKE-Restart and CYCLONE-Restart on the 30-dimensional test problems with large numbers of local minima. The averages are taken for 30 trials corresponding to 30 different starting points. Error bars represent 95% t-confidence intervals for the mean.

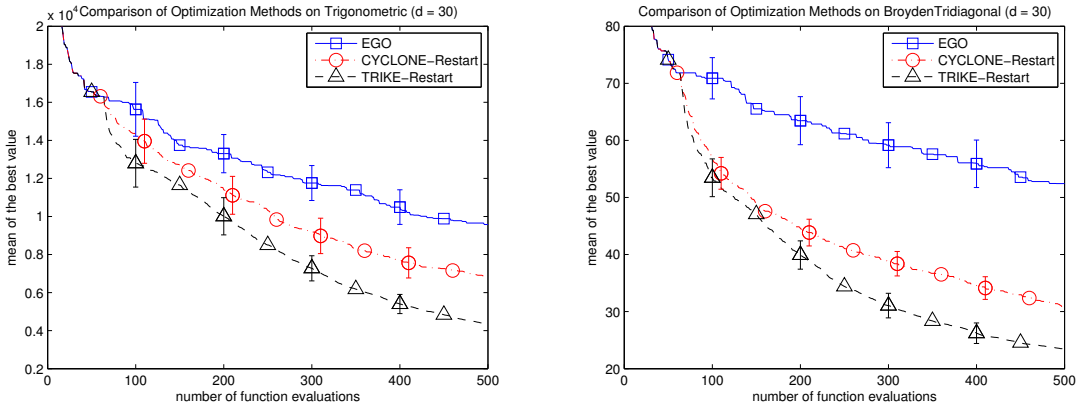

(a) (b)

Figure D.3. Average progress curves of TRIKE-Restart and CYCLONE-Restart on the higher-dimensional test problems with relatively few local minima. The averages are taken for 30 trials corresponding to 30 different starting points. Error bars represent 95% t-confidence intervals for the mean.

Appendix E. Sensitivity analysis

Figure E.1 shows the performance profiles for TRIKE-Restart with the three different values of η on the 18 lower-dimensional test problems (Figure E.1(a)) and on the 10 higher-dimensional test problems (Figure E.1(b)). The values of η include the default value of $\eta = 1$ used in the earlier comparisons. The performance profiles are calculated at 300 function evaluations for the lower-dimensional problems and at 500 function evaluations for the higher-dimensional problems.

Figure E.2 shows the performance profiles for CYCLONE-Restart with the three different search patterns on the 18 lower-dimensional test problems (Figure E.2(a)) and on the 10 higher-dimensional test problems (Figure E.2(b)). As before, the performance profiles are calculated at 300 function evaluations for the lower-dimensional problems and at 500 function evaluations for the higher-dimensional problems.

References

Dixon, L. C. W., and G. Szegö. 1978. "The global optimization problem: An introduction." In *Towards Global Optimization 2*, edited by L. C. W. Dixon and G. Szegö (1–15). Amsterdam: North-Holland.

Moré, J., B. Garbow, and K. Hillstrom. 1981. "Testing unconstrained optimization software." *ACM Transactions on Mathematical Software* 7 ([**AQ17**]): 17–41.[**AQ8**]

Regis, R. G., and C. A. Shoemaker. 2013. "A quasi-multistart framework for global optimization

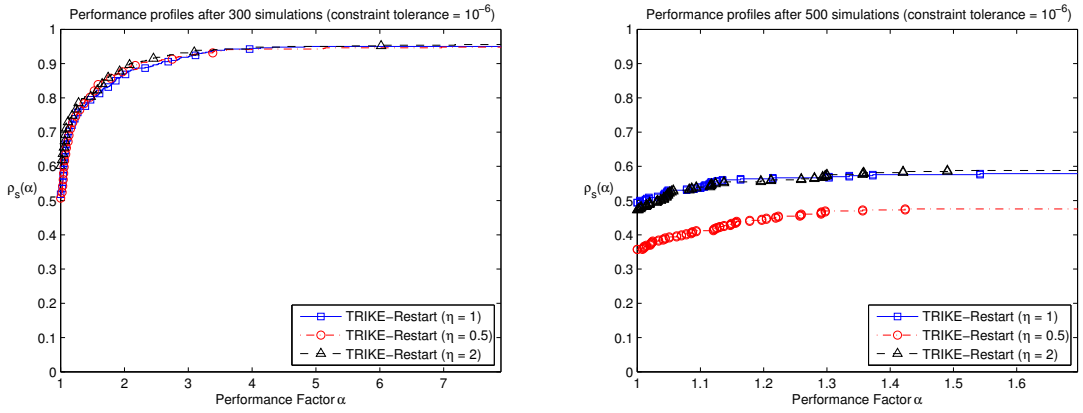

(a) (b)

Figure E.1. Performance profiles for TRIKE-Restart with different values of the parameter η on: (a) the 18 lower-dimensional test problems; and (b) the 10 higher-dimensional test problems; $\tau = 0.01$.

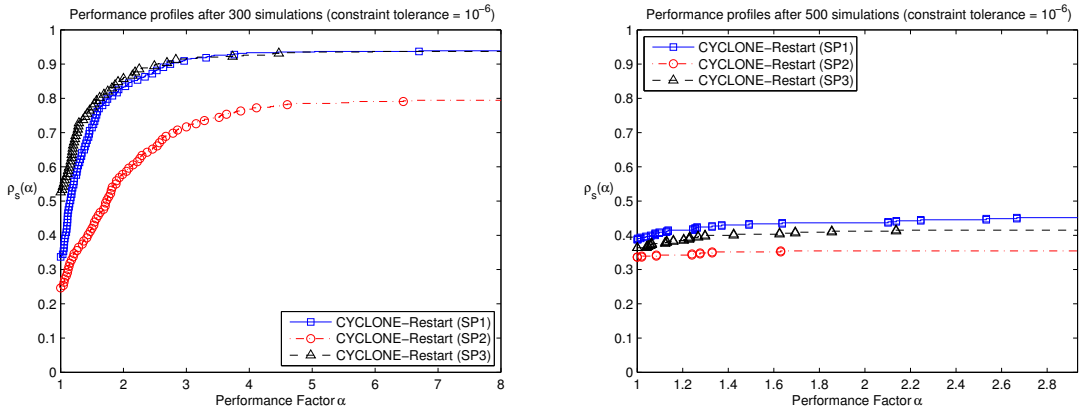

(a) (b)

Figure E.2. Performance profiles for CYCLONE-Restart with different search patterns on: (a) the 18 lower-dimensional test problems; and (b) the 10 higher-dimensional test problems; $\tau = 0.01$.

of expensive functions using response surface models." *Journal of Global Optimization* 56 (4): 1719–1753.

Schoen, F. 1993. "A wide class of test functions for global optimization." *Journal of Global Optimization* 3 ([**AQ18**]): 133–137.

Viana, F. A. C., R. T. Haftka, and L. T. Watson. 2013. "Efficient global optimization algorithm assisted by multiple surrogate techniques." *Journal of Global Optimization* 56 (2): 669–689.[**AQ9**]

Yoon, J.-H., and C. A. Shoemaker. 1999. "Comparison of optimization methods for ground-water bioremediation." *Journal of Water Resources Planning and Management* 125 ([**AQ19**]): 54–63.